

# Analyzing (Th-<sup>233</sup>U-<sup>235</sup>U)O<sub>2</sub> fuel performance in various assembly configurations: A comparative neutronic study

Fadi El Banni<sup>1</sup>, Bogbe L. H. Gogon<sup>2</sup>, Ouadie Kabach<sup>3</sup>, El Mahjoub Chakir<sup>3</sup>

<sup>1</sup> IREN, Nangui Abrogoua University, Abidjan, Cote d'Ivoire

<sup>2</sup> LASMES, SSMT, Félix Houphouët Boigny University, Abidjan, Cote d'Ivoire

<sup>3</sup> LPMS, Faculty of Sciences, Ibn Tofail University, Kenitra, Morocco

Corresponding author: Ouadie Kabach ([ouadie.kabach10@gmail.com](mailto:ouadie.kabach10@gmail.com))

Academic editor: Oleg Tashlykov ♦ Received 14 April 2024 ♦ Accepted 23 July 2024 ♦ Published 2 August 2024

Citation: El Banni F, Gogon BLH, Kabach O, Chakir EM (2024) Analyzing (Th-<sup>233</sup>U-<sup>235</sup>U)O<sub>2</sub> fuel performance in various assembly configurations: A comparative neutronic study. Nuclear Energy and Technology 10(3): 169–178. <https://doi.org/10.3897/nucet.10.125376>

## Abstract

This article investigates alternate fuel options for Pressurized Water Reactors (PWRs), focusing on thorium use to address safety, efficiency, and waste issues associated with standard UO<sub>2</sub> fuel. Challenges in thorium utilization, such as the lack of a fissile isotope, are handled using approaches such as homogeneous mixtures and heterogeneous arrangements, promoting the exploration of (Th-<sup>233</sup>U-<sup>235</sup>U)O<sub>2</sub> fuel in various assembly configurations. According to recent research, the annular dual-cooled assembly design has promising results in terms of fuel efficiency and safety while lowering the requirement for higher fissile enrichment levels. Studies additionally demonstrate that annular dual-cooled duplex fuel configurations can produce higher discharge burnup and lower power peaking factors than traditional UO<sub>2</sub> fuel. The purpose of this work is to analyze and compare the performance of (Th-<sup>233</sup>U-<sup>235</sup>U)O<sub>2</sub> fuel in various configurations against conventional UO<sub>2</sub> fuel, focusing on key characteristics such as reactivity change, criticality, discharge burnups, and reactivity feedback coefficients.

## Keywords

Thorium-based nuclear fuel, PWR, Dual-cooled annular assembly, Neutronic evaluation, Criticality, Safety coefficients

## Introduction

PWRs predominantly utilize low-enriched uranium dioxide (LEU) fuels; however, numerous alternative fuel options have been proposed over decades to address various concerns. These include enhancing safety parameters, developing fuels resilient to severe operating and irradiation conditions, minimizing nuclear waste, and increasing burnup efficiency. Among these alternatives, there's a growing interest in exploring the potential of thorium utilization. However, utilizing thorium poses challenges. For instance,

pure ThO<sub>2</sub> lacks a fissile isotope, rendering it incapable of initiating a fission chain reaction in thermal reactors. Consequently, the initial utilization of thorium necessitates the incorporation of fissile material from the uranium cycle. In response to this challenge, numerous studies have investigated methods to incorporate thorium, either through different fuel mixtures or innovative fuel assembly arrangements (Galahom 2018; Galahom et al. 2021).

In general, the approaches for introducing fissile material to produce a thorium-based fuel are well recognized, including homogeneous mixtures and heterogeneous

arrangements (Du Toit et al. 2024). The fuel used in the homogeneous configuration is a mix of thorium and fissile material, such as uranium oxide (UO<sub>2</sub>). Still, this technique demonstrated that the poor neutronic property would increase fuel cost over the cycle, and such a method requires higher <sup>235</sup>U enrichment to match the normal cycle length in PWR. The aforementioned heterogeneous (i.e. seed & blanket) structure incorporates distinct classes of fissile material and thorium at any fuel level: pellet, pin, or assembly (Uguru et al. 2021). This spatial separation of fissile material and thorium has the potential to improve the effectiveness of new fissile breeding (i.e. <sup>233</sup>U) and easier its extraction during reprocessing. It is also recommended since this strategy can be used on a small or large basis. Uranium and thorium are separated within a fuel assembly or a fuel rod using a micro-heterogeneous configuration, such as a duplex fuel rod. In contrast, the macro-heterogeneous fuel concept aims for spatial separation at the fuel assembly level (Galahom 2020).

Recent research indicates that using (Th-<sup>233</sup>U-<sup>235</sup>U)<sub>2</sub> fuel in an annular dual-cooled 13 × 13 assembly design can be a feasible alternative to traditional solid UO<sub>2</sub> in homogeneous mixes (Benrhnia et al. 2022; Bouassa et al. 2023; Lkouz et al. 2023a, 2023b; Kabach et al. 2024). This fuel composition, which combines <sup>232</sup>Th, <sup>233</sup>U, and recovered <sup>235</sup>U, seeks to capitalize on the advantages of both <sup>233</sup>U and <sup>235</sup>U. This technique reduces the need for higher fissile enrichment and compensates for the reduced delayed neutron percentage and negative moderator temperature coefficients, which are principally influenced by <sup>233</sup>U (El Banni et al. 2022). Furthermore, the dual-cooled assembly design enhances the cooling of the fuel rods, mitigating the risk of overheating and cladding damage. This contributes to accident prevention and enhances reactor safety. The enhanced cooling of the fuel rods in the dual-cooled design can extend fuel lifetimes by reducing susceptibility to damage from overheating, thus allowing for higher power density and increased reactor efficiency (Hejzlar and Kazimi 2007; Yang et al. 2009; Shin et al. 2012; Deng et al. 2016). Research outcomes indicate that incorporating <sup>233</sup>U and <sup>235</sup>U with <sup>232</sup>Th enhances fuel burnup and augments the net delayed neutron fraction, while also introducing negative feedback into the overall moderator temperature coefficient. Moreover, (Th-<sup>233</sup>U-<sup>235</sup>U)<sub>2</sub> fuel yields lower levels of <sup>239</sup>Pu and minor actinide concentrations.

Previous studies have also looked into the advantages of annular dual-cooled fuel and duplex fuel configurations in a Westinghouse SMR assembly, which is a scaled-down version of the AP1000 reactor. These investigations intended to improve the present performance criteria for such reactor types. To account for the dual-cooled feature, the study investigates both duplex configurations: ThO<sub>2</sub> in the inner region and UO<sub>2</sub> in the outer region, as well as UO<sub>2</sub> in the inner region and ThO<sub>2</sub> in the outer region (El Kheiri et al. 2023; Kheiri et al. 2023). This study found that annular duplex fuels can produce higher discharge burnup than annular UO<sub>2</sub> fuel, despite having approximately comparable reactivity values at the beginning of

the cycle. Annular duplex fuels also have lower power peaking factors, which are beneficial for reactor operation.

Given these considerations, one of the main objectives of this paper is to analyze and comprehend the performance of (Th-<sup>233</sup>U-<sup>235</sup>U)<sub>2</sub> fuel in three different configurations: simple annular dual-cooled, dual-cooled macro-heterogeneous, and dual-cooled micro-heterogeneous. This examination will be carried out by comparing them to conventional LEU-UO<sub>2</sub> fuel. Key characteristics to assess include reactivity change, criticality time, discharge burnups, power distribution, delayed neutron fractions, and reactivity feedback coefficients.

## Materials and methods

### Dimensions of reference and suggested assemblies

In this study, we examine two distinct fuel types, both possessing the same cumulative enrichment level of 4.95 wt. %, across five proposed fuel assembly (FA) configurations. The first fuel option is UO<sub>2</sub>, while the second comprises a composite of <sup>232</sup>Th, <sup>233</sup>U, and <sup>235</sup>U, forming (Th-<sup>233</sup>U-<sup>235</sup>U)<sub>2</sub> fuel. Table 1 outlines the characteristics of these investigated fuels.

**Table 1.** The main properties of the investigated fuel types (Kabach et al. 2024).

Fuel	Density	Fertile	Fissile	Enrichment
UO <sub>2</sub>	10.53 (g/cm <sup>3</sup> )	<sup>238</sup> U	<sup>235</sup> U	4.95 wt.% ( <sup>235</sup> U)
(Th- <sup>233</sup> U- <sup>235</sup> U) <sub>2</sub>	9.54 (g/cm <sup>3</sup> )	<sup>232</sup> Th	<sup>233</sup> U & <sup>235</sup> U	2.475 wt.% ( <sup>233</sup> U) 2.475 wt.% ( <sup>235</sup> U)

A single fuel assembly based on the Westinghouse-designed AP1000 was taken as the reference design (FA-1). This assembly contains a 17 × 17 grid, accommodating 264 fuel rod positions, 24 guide thimbles for control rods, and one central guide thimble for core instrumentation. The fuel rods are with UO<sub>2</sub> fuel with 95.5% theoretical density, each with a radius of 0.409575 cm. The fuel pellets are separated from the cladding by a 0.008 cm gap. The cladding is made of 0.06 cm thick Zirlo™, and the fuel rods are pitched at 1.26 cm (Schulz 2006).

Given the objectives outlined in the introduction, the primary focus of this paper is to analyze and understand the performance of (Th-<sup>233</sup>U-<sup>235</sup>U)<sub>2</sub> fuel across various configurations. Prior research suggests that utilizing (Th-<sup>233</sup>U-<sup>235</sup>U)<sub>2</sub> fuel in dual-cooled assembly designs enhances fuel rod cooling, thereby mitigating the risk of overheating and cladding damage (Benrhnia et al. 2022; Bouassa et al. 2023). Building upon the previous research, a 13 × 13 annular dual-cooled assembly was designed and loaded with (Th-<sup>233</sup>U-<sup>235</sup>U)<sub>2</sub> fuel in this study. Three methods were employed: in FA-2 and FA-3, both fuels were distributed homogeneously. FA-4 uses a macro-heterogeneous concept, with the assembly divided into a Blanket region fueled by (Th-<sup>233</sup>U-<sup>235</sup>U)<sub>2</sub> and a Seed region fueled by UO<sub>2</sub>. However, FA-5 uses a micro-heterogeneous concept,

with the inner zone fueled by  $\text{UO}_2$  and the outer by  $(\text{Th-}^{233}\text{U-}^{235}\text{U})\text{O}_2$ . The geometric configurations of the assemblies are illustrated in Fig. 1. Supplementary structural material data can be found in Tables 2, 3, while Table 4 offers a comprehensive overview of the cases analyzed in the neutronic study. Additionally, Table 5 shows detailed mass compositions of the different fuel assemblies at BOC.

**Used codes**

The methodology employed in this study builds upon the approaches used in prior research (Benrhnia et al. 2022; Bouassa et al. 2023; Lkouz et al. 2023a, 2023b; Kabach et al. 2024). Both the DRAGON Version 5 and MCNP codes were utilized throughout this investigation. DRAGON code, an open-source package developed by École Polytechnique

**Table 2.** Geometrical specification of rod and guide in study assemblies (Benrhnia et al. 2022; El Kheiri et al. 2023).

Parameter	Solid	Dual-cooled	Dual-cooled duplex
Rod lattice pitch (cm)	1.260	1.648	1.648
Inner clad inner radius (cm)	-	0.431650	0.431650
Inner clad outer radius (cm)	-	0.488650	0.488650
Inner helium gap outer radius (cm)	-	0.494850	0.494850
Fuel 1 outer radius (cm)	0.409575	0.705150	0.598697
Fuel 2 outer radius (cm)	-	-	0.705150
Outer helium gap outer radius (cm)	0.417750	0.711350	0.711350
Outer clad outer radius (cm)	0.474750	0.768350	0.768350
Total fuel area per rod (cm <sup>2</sup> )	0.527007	0.792812	0.792812
Guide tube			
Guide tube inner radius (cm)	0.56	0.71	0.71
Guide tube outer radius (cm)	0.60	0.77	0.77

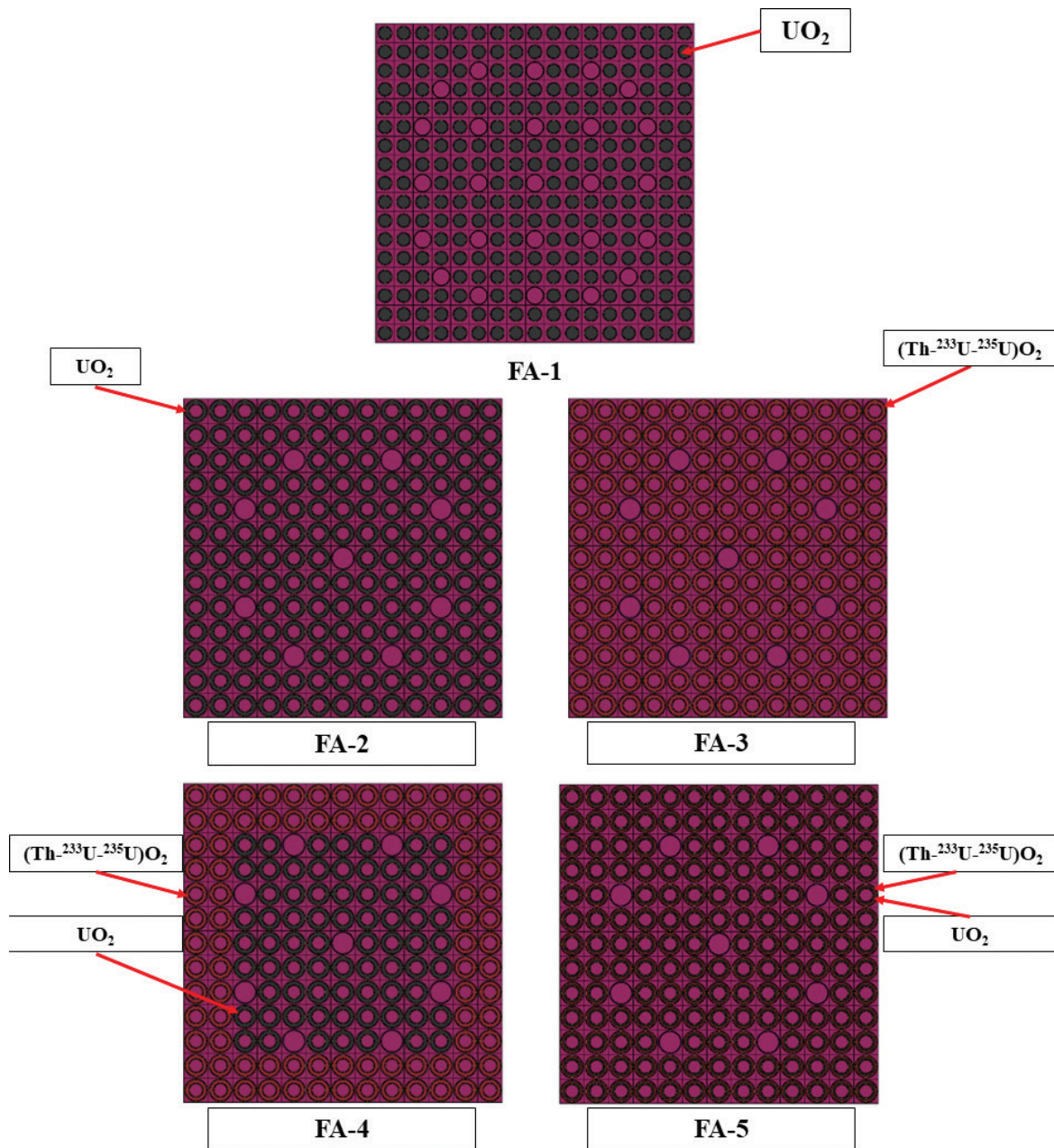


**Figure 1.** Horizontal cross-section of the suggested assembly models.

**Table 3.** Other data for reference assemblies.

Zone	Parameter	Value
Cladding	Material	Zirlo™
	Density	6.50 g/cm <sup>3</sup>
Gap	Gap material	Helium
	Gap density at 600 K	0.012 g/cm <sup>3</sup>
Moderator	Material	Light water
	Density at 573 K	0.721 g/cm <sup>3</sup>
Guide tube cladding	Material	Stainless Steel type 304
	Density	8.03 g/cm <sup>3</sup>

**Table 4.** Considered cases for the neutronic study.

Case Name	Configuration and compositions
FA-1	Solid (17 × 17) with 264 UO <sub>2</sub> fuel rods per assembly.
FA-2	Dual-cooled (13 × 13) with 160 UO <sub>2</sub> fuel rods per assembly.
FA-3	Dual-cooled (13 × 13) with 160 (Th- <sup>233</sup> U, <sup>235</sup> U)O <sub>2</sub> fuel rods per assembly.
FA-4	Dual-cooled (13 × 13) with 72 UO <sub>2</sub> and 88 (Th- <sup>233</sup> U, <sup>235</sup> U)O <sub>2</sub> fuel rods per assembly in macro-heterogeneous configuration.
FA-5	Dual-cooled (13 × 13) with 160 fuel rods per assembly in micro-heterogeneous configuration (UO <sub>2</sub> & (Th- <sup>233</sup> U, <sup>235</sup> U)O <sub>2</sub> ).

**Table 5.** Mass compositions of the different fuel assemblies at BOC.

Case Name	Nuclide	Mass (kg)
FA-1	<sup>235</sup> U	27.25
	<sup>238</sup> U	523.30
FA-2	<sup>235</sup> U	24.85
	<sup>238</sup> U	477.20
FA-3	<sup>232</sup> Th	431.40
	<sup>233</sup> U	11.23
	<sup>235</sup> U	11.23
FA-4	<sup>232</sup> Th	237.30
	<sup>233</sup> U	6.18
	<sup>235</sup> U	17.36
	<sup>238</sup> U	214.70
FA-5	<sup>232</sup> Th	237.30
	<sup>233</sup> U	6.18
	<sup>235</sup> U	17.36
	<sup>238</sup> U	214.70

de Montréal, is employed to solve the neutron transport equation at the assembly level, employing deterministic methods like the collision probability method, discrete ordinate method, or method of characteristic (Hébert 2008; Marleau et al. 2021). DRAGON utilizes various modules for different functions associated with solving transport or diffusion equations, including LIB, GEO, EXCELT, MC-CGT, SHI, ASM, FLU, EVO, and EDI. For this study, the cross-section library ENDFB-VIII ref.0 (SHEM-361) accessible via the download page was utilized.

Additionally, MCNP, a Monte Carlo code, was employed in this study to verify and validate the DRAGON depletion results, particularly in terms of the eigenvalue ( $k_{inf}$ ). MCNP, utilizing the Monte Carlo probabilistic method, is designed to simulate the transport of large particles such as neutrons, photons, and electrons in complex geometric models (Werner 2017). The simulations in this

research were conducted using a custom-developed library based on ENDFB-VIII.0 nuclear data (Brown et al. 2018; Kabach et al. 2019, 2021). The MCNP burnup runs comprised 80,000 neutrons per cycle with 150 inactive and 150 active cycles for each time step, resulting in a maximum uncertainty of 19 pcm.

### Calculation methodology

As per available literature, large PWRs typically exhibit neutron leakage levels ranging from 3% to 4%, with the initial reactivity showing an approximately linear variation. In the present study, the constructed models include reflective boundary conditions on outer surfaces, hence neglecting neutron leakage in the eigenvalue calculation. To address neutron leakage, a 3% reactivity correction is applied. As a result, the single-batch discharge burnup is adjusted to yield a  $k_{inf}$  value of  $\approx 1.03$ . The Linear Reactivity Model (LRM) is then used to convert the single-batch discharge burnup into that of a three-batch core (Burns et al. 2020; Akter et al. 2021; Hossain et al. 2022). The relationship between the discharge burnup for an  $N_{RB}$ -batch core ( $B_{Discharge}$ ), the single-batch discharge burnup ( $B_{SC}$ ), and  $N_{RB}$ , the number of fuel batches in the fuel assembly shuffling scheme is given by:

$$B_{Discharge} = N_{RB} B_{NC} = \frac{2N_{RB}}{(N_{RB} + 1)} B_{SC} \quad (1)$$

The corresponding cycle lengths were calculated using the formula:

$$T_{cycle} = \frac{2}{(N_{RB} + 1)} \frac{B_{SC}}{\rho} \quad (2)$$

where  $T_{cycle}$  represents the cycle length in Effective Full Power Days (EFPDs), and  $\rho$  is the specific power density of 40 kW/kg. In our cases, the discharge burnup and cycle length for each fuel model were modeled as calculated from the LRM under the assumption of a 3-batch core with 3% neutron leakage (Kabach et al. 2024).

The dynamics of a nuclear reactor during normal operation can be approximated by considering the number of delayed neutron emissions resulting from the decay of fission products. Safety parameters for reactors predominantly fueled by UO<sub>2</sub> include a higher ratio of effective delayed neutrons ( $\beta_{eff}$ ), which is crucial for licensing operations (Washington 2016). Since  $\beta_{eff}$  is influenced by the type of fuel used—whether fissile or fertile—it's essential to assess how altering or changing the fuel type affects this parameter throughout burnup. In this study, MCNP, with options invoked on the KOPTS card, is utilized to compute  $\beta_{eff}$  (Werner 2017). This approach allows for the analysis of the impact of fuel variations on reactor dynamics and safety characteristics as burnup progresses.

Fuel and moderator temperature coefficients are two critical reactivity coefficients. The fuel temperature coefficient (FTC) is defined as the fractional change in  $k_{inf}$  per unit change in fuel temperature, while the moderator temperature coefficient (MTC) is defined similarly for

moderator temperature changes. In this study, FTC and MTC were evaluated at the beginning of cycle (BOC) and end of cycle (EOC) steps. The evaluated models are compared for the following temperature perturbation scenarios:

- Increasing the fuel temperature by 100 K over the baseline of 900 K.
- Increasing the moderator temperature by 20 K above the 573 K baseline.

The reactivity coefficients are then determined using Eq. (3), where  $\alpha$  represents the evaluated coefficient,  $X_1$  and  $X_2$  are the changes in the considered parameter, and  $k_1$  and  $k_2$  are the multiplication factors arising from the states  $X_1$  and  $X_2$ . These factors are multiplied by  $10^5$  to yield results in pcm (Bouassa et al. 2023).

$$\alpha = \frac{1}{X_2 - X_1} \left( \frac{k_2 - k_1}{k_2 k_1} \right) \cdot 10^5 \quad (3)$$

## Results and discussion

### Fuel burn-up

The neutronic calculations for the analyzed fuel type assemblies were conducted at a boron concentration of 0 ppm, with all control rods withdrawn. Fig. 2 depicts the  $k_{\text{inf}}$  as a function of fuel burnup for the investigated assemblies, comparing results from the DRAGON and MCNP code. The general pattern across the analyzed scenarios is consistent:  $k_{\text{inf}}$  falls dramatically during the early burnup stage due to the production of  $^{135}\text{Xe}$  and  $^{149}\text{Sm}$ , which have high absorption cross-sections.  $k_{\text{inf}}$  then decreases linearly with burnup, albeit at various rates, as a result of the burning of fissile material. According to previous studies, (Th- $^{233}\text{U}$ - $^{235}\text{U}$ ) $\text{O}_2$ -fueled models produce less  $^{135}\text{Xe}$ - and  $^{149}\text{Sm}$

than regular  $\text{UO}_2$  fuels (Benrhnia et al. 2022; Lkouz et al. 2023b; Kabach et al. 2024).

As shown in Fig. 2 and outlined in Table 6, FA-3 scenario fuel has a higher reactivity at BOC and sustains criticality longer than FA-1, despite the fuel types having the same enrichment and the total fuel volume being lowered when transitioning from solid  $17 \times 17$  to a dual-cooled  $13 \times 13$  assembly. This discrepancy can be attributed to the advantageous characteristics of  $^{233}\text{U}$  as a fissile material in a thermal reactor compared to  $^{235}\text{U}$ . Specifically,  $^{233}\text{U}$  demonstrates the lowest capture-to-fission ratio, resulting in higher neutron production per neutron absorbed in the fuel ( $\eta$ ). The  $\eta$  value for  $^{233}\text{U}$  is approximately  $2.497 \pm 0.004$ , whereas for  $^{235}\text{U}$  it is about  $2.435 \pm 0.002$  (Abdelghafar Galahom et al. 2024).

Transitioning from an all (Th- $^{233}\text{U}$ - $^{235}\text{U}$ ) $\text{O}_2$ -fueled assembly to the macro-heterogeneous (FA-4) and micro-heterogeneous (FA-5) configurations reveals distinct patterns in terms of initial reactivities and criticality, even though the total volumes occupied by  $\text{UO}_2$  and (Th- $^{233}\text{U}$ - $^{235}\text{U}$ ) $\text{O}_2$  are the same for FA-4 and FA-5 (see Tables 2, 4). FA-4 sustains criticality 0.24% longer than FA-1 and 9.77% longer than FA-2, despite having lower reactivity at BOC than FA-1. However, the criticality is reduced by 5.41% compared to FA-1, primarily due to the decreased concentration of  $^{233}\text{U}$ . FA-5 sustains criticality for a short-

**Table 6.** Comparison of  $k_{\text{inf}}$  at BOC and EOC, and the single-batch discharge burnup ( $B_{\text{sc}}$ ).

Case Name	$k_{\text{inf}}$ (BOC)		$k_{\text{inf}}$ (EOC)		$B_{\text{sc}}$ (MWd/kg)	
	DRAGON	MCNP	DRAGON	MCNP	DRAGON	MCNP
FA-1	1.41672	1.41245	0.89381	0.90146	38.38	39.39
FA-2	1.37707	1.37474	0.89087	0.89803	34.73	35.82
FA-3	1.41836	1.41753	0.91448	0.92239	40.67	42.00
FA-4	1.39207	1.39239	0.90579	0.91291	38.48	39.81
FA-5	1.31661	1.31482	0.91461	0.92149	33.93	35.14

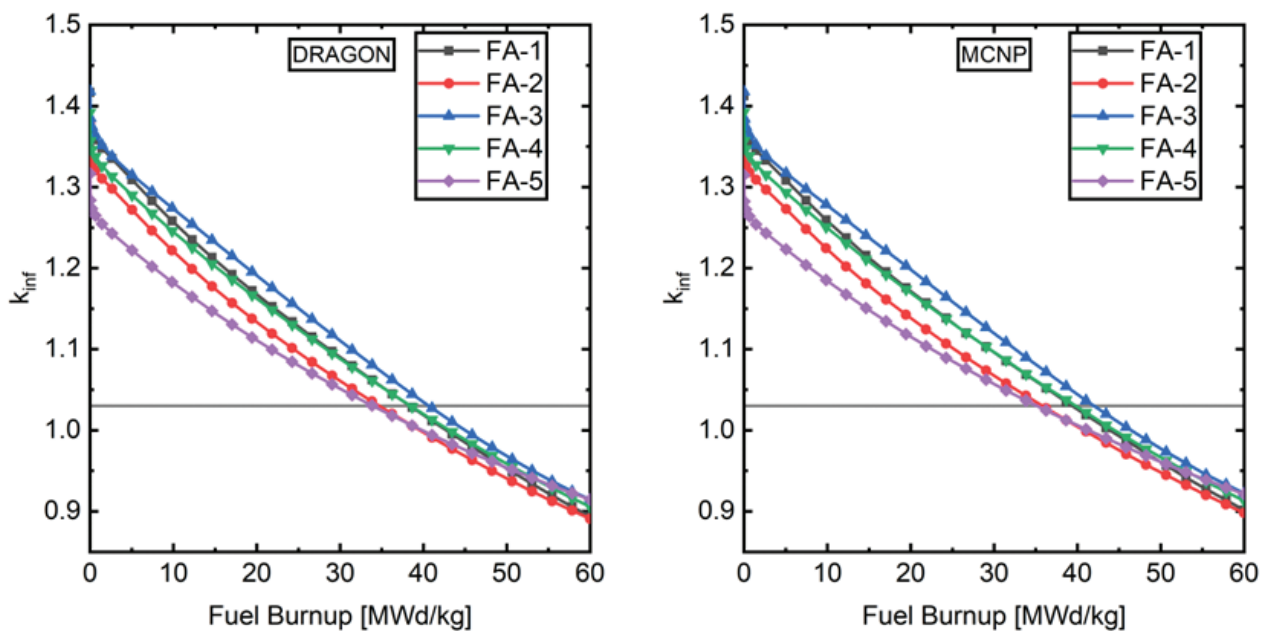


**Figure 2.** Infinite multiplication factor trend for the analyzed assembly models.

er duration than all other cases, which can be attributed to the duplex design's enhanced self-shielding effect.

As previously mentioned, the LRM was utilized to accurately represent key cycle parameters, including cycle burnup, discharge burnup, and cycle length. The results are visually depicted in bar chart representations in Figs 3–5. Fuel cycle parameters for FA-2 exceeded those for UO<sub>2</sub> assemblies (i.e. FA-1 and FA-2), as anticipated. Similarly, the FA-4 case exhibited enhanced fuel cycle parameters compared to UO<sub>2</sub> assemblies. Given that cycle burnup, discharge burnup, and cycle length are linked to the single batch criticality period, it follows that a decrease in the criticality in the FA-5 case leads to reductions in the values of these parameters as well.

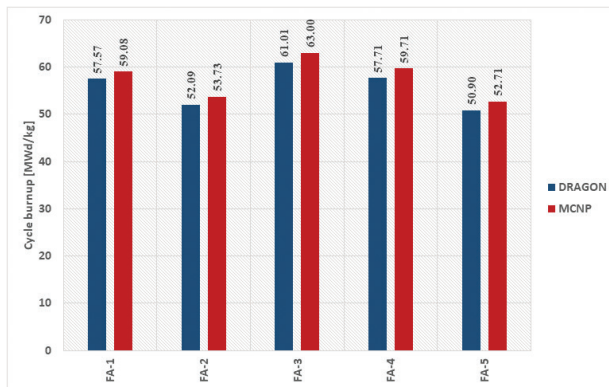


Figure 3. Comparison of cycle burnup.

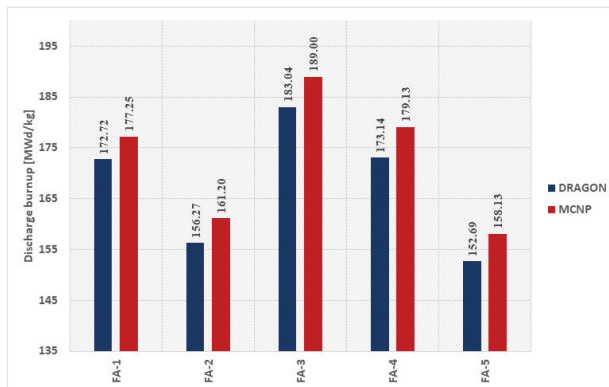


Figure 4. Comparison of discharge burnup.

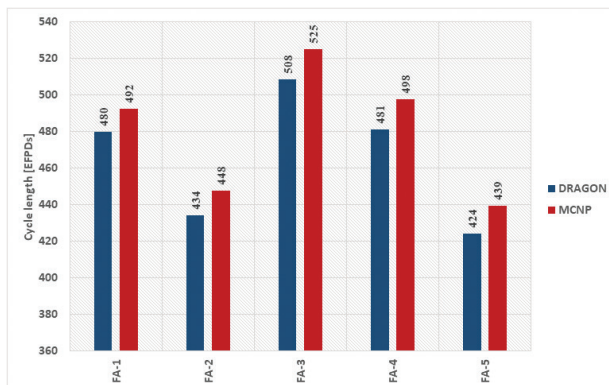


Figure 5. Comparison of cycle length.

## Fissile inventory ratio

The fissile inventory ratio (FIR) is a crucial metric for reactor operation and is an effective means to evaluate a reactor's breeding capability. This ratio represents the proportion of the fuel's fissile content to its initial fissile content, serving as an indicator of the conversion ratio. The fissile nuclei considered in this study to measure the conversion ratio include <sup>233</sup>U, <sup>235</sup>U, <sup>239</sup>Pu, and <sup>241</sup>Pu (Galahom 2019). Additionally, <sup>233</sup>Pa and <sup>233</sup>Np were considered fissile materials to calculate the FIR because they will eventually decay into <sup>233</sup>U and <sup>239</sup>Pu, respectively, after the assembly has been discharged (Alam et al. 2019).

Fig. 6 illustrates the variation of the FIR with burnup. It is observed that the ratio in UO<sub>2</sub>-based assemblies is smaller compared to (Th-<sup>233</sup>U-<sup>235</sup>U)<sub>2</sub>-based assemblies. Interestingly, the FIR for FA-5 is higher, with the difference increasing with burnup. This is attributed to the use of a micro-heterogeneous “duplex” configuration, which allows for a higher conversion rate of fertile material into fissile material. Furthermore, the double cooling system enables a greater moderator volume, enhancing neutron thermalization. This improvement in neutron utilization results in a better conversion of fertile material to fissile material, as shown in Fig. 7.

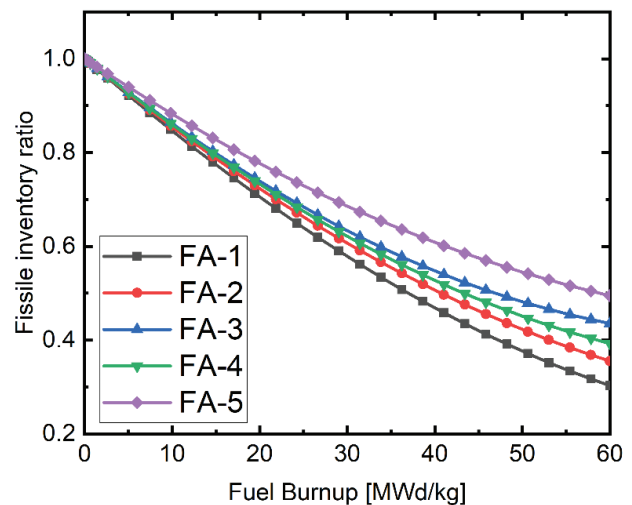


Figure 6. Variation of FIR with burnup for the different investigated assembly types.

## Neutron spectra profiles

The neutron spectrum is influenced by the balance between neutron moderation and absorption. Fig. 8 illustrates the neutron flux per unit lethargy, the spectra are plotted using the DRAGLIB\_SHEM-361-group energy structure. The micro-heterogeneous configuration (FA-5) results in a harder neutron spectrum due to the increased self-shielding effect inherent in its duplex design. Since a harder spectrum facilitates the efficient conversion of fertile material to fissile material, the FIR values are higher for FA-5, as depicted in Fig. 6.

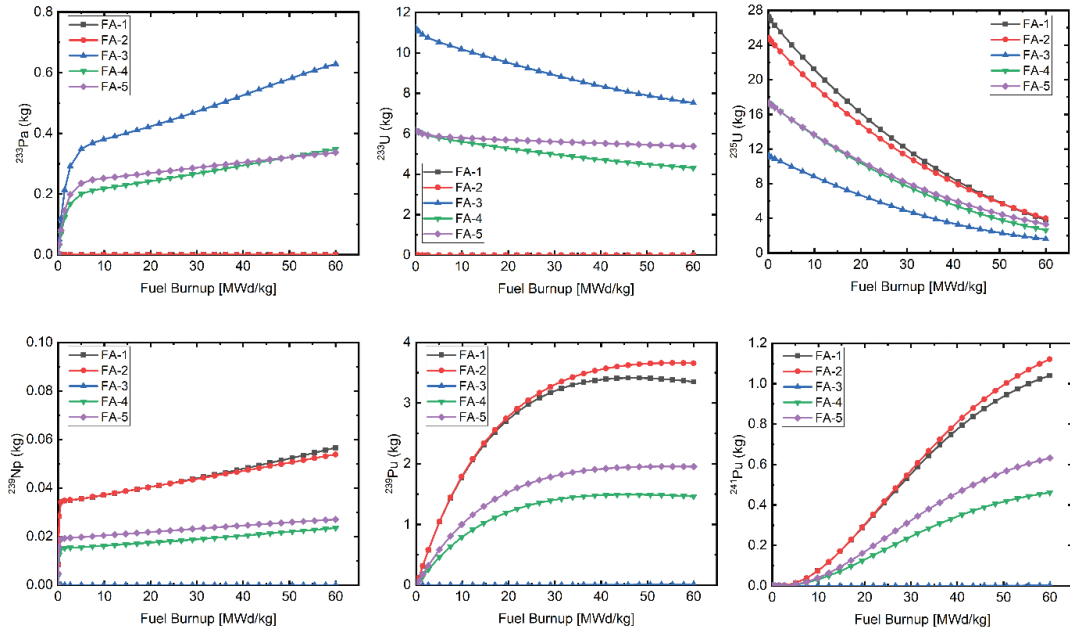


Figure 7. Variation of mass (in kg) of  $^{233}\text{Pa}$ ,  $^{233}\text{U}$ ,  $^{235}\text{U}$ ,  $^{239}\text{Np}$ ,  $^{239}\text{Pu}$ , and  $^{241}\text{Pu}$  with burnup.

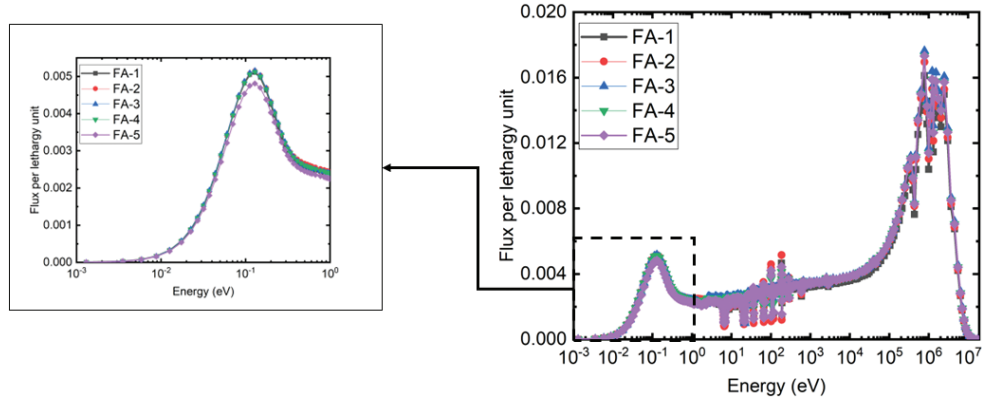


Figure 8. Normalized neutron spectra.

**Radial power distribution**

Fig. 9 depicts the relative pin power of the evaluated assembly cases at both BOC and EOC. The numerical values show the pin power ratio to the assembly’s average pin power, with red numbers representing hot channels. The maximum pin powers at BOC and EOC for FA-3 are lower when compared to FA-1 and FA-2. However, using the macro-heterogeneous assembly (FA-4) presents a considerable issue because the maximum pin power increases due to EOC. This is linked to increased plutonium production in the  $\text{UO}_2$  region, which creates a power imbalance between the blanket and seed regions. In contrast, the micro-heterogeneous assembly (FA-5) maintains constant pin power values throughout the burnup cycle. This shows that the annular duplex fuel design provides safety benefits, as the fuel temperature remains lower than in other cases.

**Delayed neutrons**

Changes in  $\beta_{\text{eff}}$  values with fuel burnup are depicted in Fig. 10. It is expected that  $(\text{Th}-^{233}\text{U}-^{235}\text{U})\text{O}_2$ -based assemblies

would exhibit lower  $\beta_{\text{eff}}$  values at BOC and during burnup compared to all  $\text{UO}_2$  assemblies, as  $^{233}\text{U}$  has a lower delayed neutron fraction than  $^{235}\text{U}$  (Benrhnia et al. 2022). However, despite this expectation, the addition of  $\text{UO}_2$  improves the  $\beta_{\text{eff}}$  values, as evident in the FA-4 and FA-5 cases compared to FA-3. The decrease in  $\beta_{\text{eff}}$  values with burnup observed in FA-4 and FA-5 cases is also observed in  $\text{UO}_2$  assemblies, attributed to the production of  $^{239}\text{Pu}$ , which has a lower delayed neutron fraction. Nevertheless, it is worth noting that the favorable fuel temperature coefficients discussed below may compensate for the lower delayed neutron fraction.

**Reactivity feedback coefficients**

Fig. 11 illustrates the FTC values for the investigated assembly models at BOC and EOC. The illustration shows highly negative FTC values, with a greater influence shown in  $(\text{Th}-^{233}\text{U}-^{235}\text{U})\text{O}_2$  assemblies than in  $\text{UO}_2$  assemblies, notably at BOC. Additionally, the FTC values for FA-5 followed by FA-4 are more negative than in the other cases. The aforementioned phenomenon can be explained by the increased influence of the Doppler effect, which is amplified when

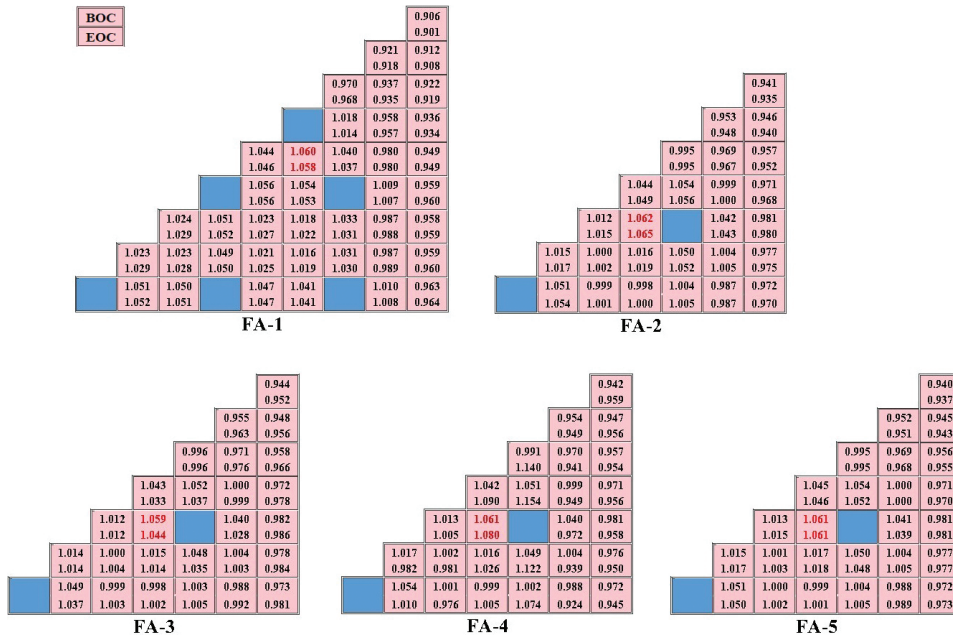


Figure 9. Radial power factors distribution for the studied cases at BOC and EOC.

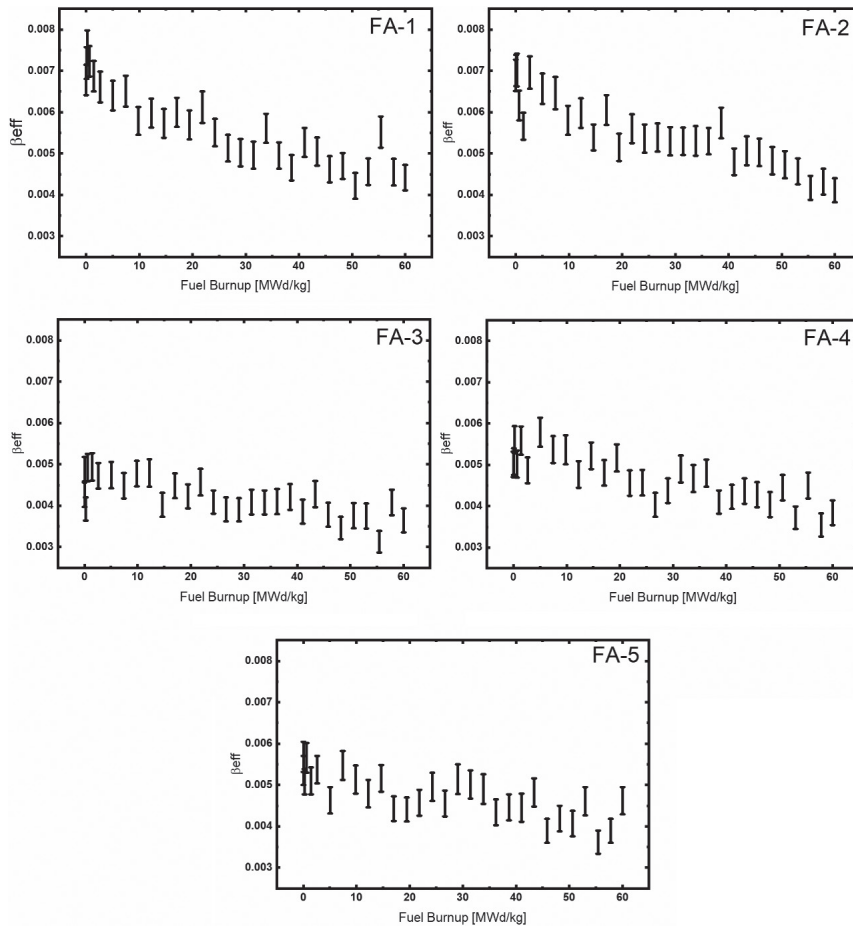


Figure 10. Change in  $\beta_{eff}$  with fuel burnup.

<sup>232</sup>Th is coupled with <sup>238</sup>U. Furthermore, FA-5 has higher negative FTC values than FA-4 because of the increased self-shielding effect inherent in the duplex design.

Previous research studies have shown that using <sup>233</sup>U as fissile material in LWRs is a problem because of its potential to produce lower negative or even positive MTC

values. This behavior is essentially related to the epithermal fission resonance cross-section of <sup>233</sup>U at higher neutron temperatures. However, as shown in Fig. 12, the combination of (Th-<sup>233</sup>U-<sup>235</sup>U)<sub>2</sub> and UO<sub>2</sub> in the assembly improves MTC values in FA-4 and FA-5, with a stronger influence in FA-5 due to the greater self-shielding effect



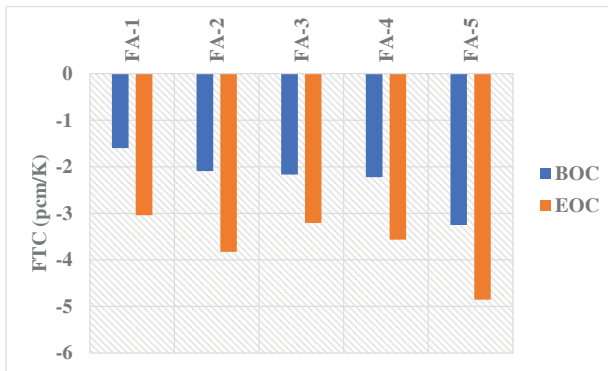


Figure 11. FTC at BOC and EOC for the analyzed assembly cases.

in the duplex design. As a result, based on the obtained FTC and MTC values, FA-5 provides increased stability and control in terms of reactivity feedback coefficients.

## Conclusion

The increasing need for thorium-based fuel in PWRs highlights the significance of exploring novel approaches for enhancing nuclear energy performance. One such approach includes combining  $^{233}\text{U}$  and  $^{235}\text{U}$  with  $^{232}\text{Th}$  to create  $(\text{Th}-^{233}\text{U}-^{235}\text{U})\text{O}_2$  fuel. This study aimed to compare the neutronic safety properties of  $(\text{Th}-^{233}\text{U}-^{235}\text{U})\text{O}_2$  fuel in various configurations within a dual-cooled annular  $13 \times 13$  assembly. The study examined criticality, cycle length parameters, power distributions, delayed neutron fractions, and reactivity feedback coefficients for various assembly configurations. The study focused on the simple annular dual-cooled (FA-3), dual-cooled macro-heterogeneous (FA-4), and dual-cooled micro-heterogeneous (FA-4) configurations of  $(\text{Th}-^{233}\text{U}-^{235}\text{U})\text{O}_2$  with  $\text{UO}_2$ .

The findings show that the micro-heterogeneous configuration exhibits lower criticality and cycle length compared to all- $\text{UO}_2$  assemblies. In contrast, the macro-heterogeneous design has higher criticality and cycle parameters than all- $\text{UO}_2$  assemblies. However, radial pin power data showed minor increases in the macro-heterogeneous assembly, resulting in power imbalances between the seed and blanket regions. On the other hand, the micro-heterogeneous assembly resulted in lower and more consistent pin power than  $\text{UO}_2$ . However, to fully

## References

- Abdelghafar Galahom A, Salah Khaliil A, Alnassar N, Reda SM (2024) Discussing the possibility of using thorium-based fuels as an alternative fuel to uranium dioxide fuel for APR-1400 reactor. *Nuclear Engineering and Design* 417: 112817. <https://doi.org/10.1016/j.nucengdes.2023.112817>
- Akter Y, Hossain Sahadath M, Reza F (2021) Assessment of the burnup characteristics of  $\text{UO}_2$  and MOX fuel in the mixed solid and annular rod configuration. *Nuclear Engineering and Design* 381: 111339. <https://doi.org/10.1016/j.nucengdes.2021.111339>
- Alam SB, Kumar D, Almutairi B, Bhowmik PK, Goodwin C, Parks GT (2019) Small modular reactor core design for civil marine propulsion using micro-heterogeneous duplex fuel. Part I: Assembly-level analysis. *Nuclear Engineering and Design* 346: 157–175. <https://doi.org/10.1016/j.nucengdes.2019.03.005>
- El Banni F, Kabach O, Boko A, Gogon BLH, Koua AA, Monnehan GA, Benchrif A, Amsil H, Chetaine A (2022) Neutronic investigation of a VVER-1200  $(\text{Th}-^{233}\text{U})\text{O}_2$  fuel assembly with protactinium oxide as a burnable absorber coated on the outer surface of the fuel rods.

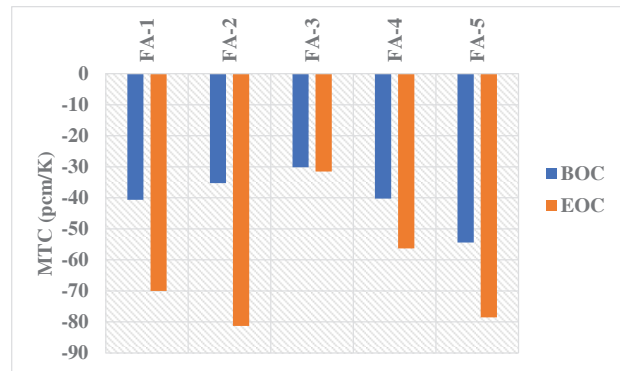


Figure 12. MTC at BOC and EOC for the analyzed assembly cases.

comprehend the impact of the fuel and assembly change, a thermal-hydraulic analysis is required. The delayed neutron fractions were also estimated, and it was found that using macro-heterogeneous or micro-heterogeneous configurations improved the net delayed neutron fraction.

In terms of moderator and fuel temperature coefficients, simulations indicated that both macro-heterogeneous and micro-heterogeneous assemblies exhibit more negative coefficients compared to the all- $(\text{Th}-^{233}\text{U}-^{235}\text{U})\text{O}_2$  assembly. Moreover, these designs demonstrated performance equivalent to traditional  $\text{UO}_2$  fuel. Therefore, the results of this paper can serve as essential data for safety analyses of PWRs with different fuel options.

## Future work

Future work will focus on detailed full-core analyses to further evaluate the safety and performance of thorium-based fuel assemblies in PWRs. Investigating future safety parameters such as reactivity control will be essential. Additionally, studies could address the thermal-hydraulic behavior and burnup characteristics of these assemblies to provide a more comprehensive understanding of their viability.

## Declaration of competing interest

The authors declare that they have no known competing financial interests or personal relationships that could have appeared to influence the work reported in this paper.

- Energy Sources, Part A: Recovery, Utilization, and Environmental Effects 44: 7650–7664. <https://doi.org/10.1080/15567036.2022.2116506>
- Benrhnia Z, Chetaine A, Kabach O, Amsil H, Benchrif A, El Banni F (2022) Neutronic and burnup characteristics of potential dual-cooled annular (Th-<sup>233</sup>U-<sup>235</sup>U)<sub>2</sub> fuel for the advanced pressurized water reactors: An assembly-level analysis. *International Journal of Energy Research* 46: 23501–23516. <https://doi.org/10.1002/er.8648>
  - Bouassa T, Kabach O, Chetaine A, Benrhnia Z, El Banni F, Saidi A (2023) Parametric neutronic analysis of different cladding options for ThO<sub>2</sub> pellet of advanced dual-cooled annular PWR assembly. *Nuclear Engineering and Design* 414: 112533. <https://doi.org/10.1016/j.nucengdes.2023.112533>
  - Brown DA, Chadwick MB, Capote R, Kahler AC, Trkov A, Herman MW, Sonzogni AA, Danon Y, Carlson AD, Dunn M, Smith DL, Hale GM, Arbanas G, Arcilla R, Bates CR, Beck B, Becker B, Brown F, Casperson RJ, Conlin J, Cullen DE, Descalle MA, Firestone R, Gaines T, Guber KH, Hawari AI, Holmes J, Johnson TD, Kawano T, Kiedrowski BC, Koning AJ, Kopecky S, Leal L, Lestone JP, Lubitz C, Márquez Damián JI, Mattoon CM, McCutchan EA, Mughabghab S, Navratil P, Neudecker D, Nobre GPA, Noguere G, Paris M, Pigni MT, Plompen AJ, Pritychenko B, Pronyaev VG, Roubtsov D, Rochman D, Romano P, Schillebeeckx P, Simakov S, Sin M, Sirakov I, Sleaford B, Sobes V, Soukhovitskii ES, Stetcu I, Talou P, Thompson I, van der Marck S, Welsch-Sherrill L, Wiarda D, White M, Wormald JL, Wright RQ, Zerle M, Žerovnik G, Zhu Y (2018) ENDF/B-VIII.0: The 8<sup>th</sup> Major Release of the Nuclear Reaction Data Library with CIELO-project Cross Sections, New Standards and Thermal Scattering Data. *Nuclear Data Sheets* 148: 1–142. <https://doi.org/10.1016/j.nds.2018.02.001>
  - Burns JR, Hernandez R, Terrani KA, Nelson AT, Brown NR (2020) Reactor and fuel cycle performance of light water reactor fuel with 235U enrichments above 5%. *Annals of Nuclear Energy* 142: 107423. <https://doi.org/10.1016/j.anucene.2020.107423>
  - Deng Y, Wu Y, Zhang D, Tian W, Qiu S, Su GH (2016) Development of a thermal-mechanical behavior coupling analysis code for a dual-cooled annular fuel element in PWRs. *Nuclear Engineering and Design* 301: 353–365. <https://doi.org/10.1016/j.nucengdes.2016.03.021>
  - Galahom AA (2018) Reducing the plutonium stockpile around the world using a new design of VVER-1200 assembly. *Annals of Nuclear Energy* 119: 279–286. <https://doi.org/10.1016/j.anucene.2018.05.022>
  - Galahom AA (2019) Improvement of the VVER-1200 Fuel Cycle by Introducing Thorium with Different Fissile Material in Blanket-Seed Assembly. *Nuclear Science and Engineering* 193: 638–651. <https://doi.org/10.1080/00295639.2018.1560757>
  - Galahom AA (2020) Investigate the possibility of burning weapon-grade plutonium using a concentric rods BS assembly of VVER-1200. *Annals of Nuclear Energy* 148: 107758. <https://doi.org/10.1016/j.anucene.2020.107758>
  - Galahom AA, Mohsen MYM, Amrani N (2021) Explore the possible advantages of using thorium-based fuel in a pressurized water reactor (PWR) Part 1: Neutronic analysis. *Nuclear Engineering and Technology* 54: 1–10. <https://doi.org/10.1016/j.net.2021.07.019>
  - Hébert A (2008) Draglib Download Page. [Available from:] <https://www.polymtl.ca/merlin/libraries.htm> [June 10, 2016]
  - Hejzlar P, Kazimi MS (2007) Annular fuel for high-power-density pressurized water reactors: Motivation and overview. *Nuclear Technology* 160: 2–15. <https://doi.org/10.13182/NT160-2-15>
  - Hossain MT, Sahadath MH, Nabila UM (2022) Neutronic and fuel cycle performance of VVER-1000 for dual cooled annular fuel with coated burnable poison. *Progress in Nuclear Energy* 145: 104139. <https://doi.org/10.1016/j.pnucene.2022.104139>
  - Kabach O, Chetaine A, Benchrif A (2019) Processing of JEFF-3.3 and ENDF/B-VIII.0 and testing with critical benchmark experiments and TRIGA Mark II research reactor using MCNPX. *Applied Radiation and Isotopes* 150: 146–156. <https://doi.org/10.1016/j.apradiso.2019.05.015>
  - Kabach O, Chakir EM, Amsil H (2024) Innovative burnable absorbers: Assessing PaO<sub>2</sub> and NpO<sub>2</sub> coatings for improved safety in (Th-<sup>233</sup>U-<sup>235</sup>U)<sub>2</sub> fuel assemblies. *Nuclear Engineering and Design* 421: 113086. <https://doi.org/10.1016/j.nucengdes.2024.113086>
  - Kabach O, Chetaine A, Benchrif A, Amsil H (2021) An inter-comparison between ENDF/B-VIII.0-NECP-Atlas and ENDF/B-VIII.0-NJOY results for criticality safety benchmarks and benchmarks on the reactivity temperature coefficient. *Nuclear Engineering and Technology* 53: 2445–2453. <https://doi.org/10.1016/j.net.2021.02.012>
  - El Kheiri O, Kabach O, Chetaine A (2023) Neutronic investigation of prospective dual-cooled micro-heterogeneous duplex fuel for small modular long-life reactors: Assembly level design and analysis. *Progress in Nuclear Energy* 160: 104680. <https://doi.org/10.1016/j.pnucene.2023.104680>
  - Kheiri OEL, Kabach O, Chetaine A (2023) Application of high-thickness integral fuel burnable absorber ZrB<sub>2</sub> in a dual-cooled micro-heterogeneous duplex fuel for small modular long-life reactor. *Annals of the University of Craiova, Physics* 33: 171–180.
  - Lkouz M, Kabach O, Chetaine A (2023a) Enhancing temperature reactivity coefficients in SMR Reactor with (Th-<sup>233</sup>U-<sup>235</sup>U)<sub>2</sub> fuel through PaO<sub>2</sub> as a burnable absorber. *Annals of the University of Craiova, Physics* 33: 181–190.
  - Lkouz M, Kabach O, Chetaine A, Saidi A, Bouassa T (2023b) Revolutionizing LWR SMR reactors: exploring the potential of (Th-<sup>233</sup>U-<sup>235</sup>U)<sub>2</sub> fuel through a parametric study. *Energy Sources, Part A: Recovery, Utilization, and Environmental Effects* 45: 10162–10175. <https://doi.org/10.1080/15567036.2023.2243859>
  - Marleau G, Hebert A, Roy R, Hébert A (2021) A User Guide for DRAGON Version5.
  - Schulz TL (2006) Westinghouse AP1000 advanced passive plant. *Nuclear Engineering and Design* 236: 1547–1557. <https://doi.org/10.1016/j.nucengdes.2006.03.049>
  - Shin CH, Chun TH, Oh DS, In WK (2012) Thermal hydraulic performance assessment of dual-cooled annular nuclear fuel for OPR-1000. *Nuclear Engineering and Design* 243: 291–300. <https://doi.org/10.1016/j.nucengdes.2011.12.010>
  - Du Toit MH, Van Niekerk F, Amirkhosravi S (2024) Review of thorium-containing fuels in LWRs. *Progress in Nuclear Energy* 170: 105136. <https://doi.org/10.1016/j.pnucene.2024.105136>
  - Uguru EH, Abdul Sani SF, Khandaker MU, Rabir MH, Karim JA, Onah DU, Bradley DA (2021) Burn-up calculation of the neutronic and safety parameters of thorium-uranium mixed oxide fuel cycle in a Westinghouse small modular reactor. *International Journal of Energy Research* 45: 12013–12028. <https://doi.org/10.1002/er.6000>
  - Washington JA (2016) The optimization of an AP1000 fuel assembly for the transmutation of plutonium and minor actinides The optimization of an AP1000 fuel assembly for the transmutation of plutonium and minor actinides. Colorado School of Mines.
  - Werner CJ (2017) MCNP® User's Manual Code Version 6.2.
  - Yang YS, Shin CH, Chun TH, Song KW (2009) Evaluation of a Dual-Cooled Annular Fuel Heat Split and Temperature Distribution. *Journal of Nuclear Science and Technology* 46: 836–845. <https://doi.org/10.1080/18811248.2007.9711593>